processes

MDPI

Article

Influence of Particle Contact Number on Triboelectric Separation Selectivity

Johann Landauer * and Petra Foerst

Chair of Process Systems Engineering, TUM School of Life Sciences Weihenstephan, Technical University of Munich, Gregor-Mendel-Straße 4, 85354 Freising, Germany; petra.foerst@tum.de

* Correspondence: johann.landauer@tum.de; Tel.: +49-8161-71-5172

Received: 22 August 2019; Accepted: 29 September 2019; Published: 9 October 2019

Abstract: Triboelectric separation is a promising technology to separate fine powders. To enable triboelectric separation for its application in industry, the impact of the process and product parameters must be examined. In this study, with regards to different wall materials in the charging step (PTFE, POM, PE, PVC, and PMMA), the influence of the powder composition of a binary starch-protein mixture with a protein content of 15 wt. %, 30 wt. % and 45 wt. % was studied. By increasing the protein content in the feed, the separation selectivity increased. No dependency of the empirical triboelectric series was determined for all powder compositions. The variation in the protein content of the initial powder and turbulent flow profiles results in a variation in the contact number of particles calculated. An increase in the contact number of particles leads to an increase in the protein content separated on the cathode, whereas the protein content on the anode is only slightly affected. These findings underpin the assumption that particle-particle interaction plays a decisive role in triboelectric charging of fine powders.

Keywords: triboelectric charging; triboelectric separation; particle-particle interaction; powder composition; contact number

1. Introduction

Triboelectric charging occurs when two surfaces come in contact and are then separated [1]. This phenomenon is called contact, surface or triboelectric charging [2,3]. While triboelectric charging is the most common expression, the subword "tribo" can be misleading as no friction is necessary to obtain charged surfaces [4]. Nevertheless, when the simplest triboelectric experiment with a balloon rubbed on hair is performed, both surfaces get charged. However, in this example, rubbing increases the number of contacts between balloon and hair and, thus, ensures sufficient contact between surfaces. This insight can be transferred to the triboelectric charging of dry powders. By dispersing powder in a gas stream high numbers of particle-particle and particle-wall collisions happen. This high interaction rate of dispersed and moved particles can be the manipulated variable for triboelectric separation of powders, since the mechanism of triboelectric charging is still unknown [5].

Triboelectric charging occurs in almost every system involving moving particles: in pneumatic conveying [6,7], fluidized beds [8], dry powder mixing [9], dust storms [10,11], or even during the formation of planets in the orbit [12] In most cases, the triboelectric charging of powders is undesirable. However, this effect can be employed as a novel separation tool for fine and dry powders [13–18]. The net amount of charge at the surface of one particle acts as a separation feature. Factors influencing triboelectric charging and separation are the chemical composition of the particles [19,20], functional groups determining surface chemistry [21], particle properties such as size, shape, and surface roughness [22–27], and electrical properties of particles as well as surrounding walls [28,29]. Furthermore, environmental conditions influence charge transfer.

Humidity [30], external electrical fields [31], and the magnitude of the contact momentum [32,33] are vital in preventing or enabling triboelectric charging. To date, the actual charging mechanisms are only partly understood [5]. Based on this background, the characterisation of influencing factors is necessary and provides an opportunity to gain further knowledge about triboelectric charging. Hence, different influencing factors must be examined for using triboelectric separation for fine powders based on their different charging properties. Hitherto, only a few studies addressed the effect of powder composition on triboelectric charging. For pharmaceutical powder mixtures, an increase in drug polymer showed a decrease in the charge to mass ratio [34]. A variation of the mixing ratio of lactose and glucose results in a twice change of sign and a charge to mass ratio of the powder. These experiments were performed for sliding particles [35].

To investigate the influence of particle-particle and particle-wall interactions on triboelectric separation, the impact of both collision types must be studied. The influence of the wall material plays a subordinated role, which was demonstrated in [36]. Particle-particle interactions might be the dominant mechanism to generate triboelectric charge in pneumatic conveyed binary particulate systems. In a binary mixture, primarily charging between different materials occurs. A single contact between two particle surfaces suffices to generate charge [29,37] or to dissipate charge [38].

Since the charging mechanism is still unknown [5] and particle-wall interaction has a subordinate role on triboelectric charging [36], it is assumed that particle-particle interactions are the main drivers of triboelectric separation. Therefore, a variation of powder composition and flow profiles are used to identify the influence of particle-particle contact numbers on triboelectric separation of fine organic powders. In this study it is hypothesised that higher particle-particle contact numbers induced by a variation of the initial powder composition and flow profiles in a turbulent flow regime improve triboelectric separation selectivity fine organic binary powder mixtures.

2. Materials and Methods

2.1. Materials

Whey protein isolate and barley starch are used as model particles and were purchased form Davisco Foods International, USA, and Altia, Finland, respectively. Whey protein isolate has a protein content of 97.6 wt. %. Barley starch has a protein content below 0.5 wt. % and starch content of 97.0 wt. %. Barley starch was classified using a wheel classifier ATP 50, Hosokawa Alpine, Germany at a deflection wheel speed of 10,000 rpm, a mass flow of 4.3 kg h^{-1}, and an air flow rate of 58 kg h^{-1}. Whey protein was ground with the same conditions as shown in [36].

2.2. Methods

2.2.1. Experimental Setup

The simple experimental setup demonstrated by Landauer et al. [36,39] was used, which consists of an exchangeable charging section and a rectangular separation chamber. A scheme of the setup is shown in Figure 1. In the charging section, a Venturi nozzle facilitates the dispersion of powders added to the gas flow. 2.5 g of powder are added manually to the gas flow during 300 ± 10 s. Since the constant feed time a continuous mass flow can be assumed. The charging tube dimensions are 10 mm in diameter and 230 mm in length. The setup enables the use of different charging sections. Five different insulators (Polytetrafluoroethylene PTFE, Polyvinylchloride PVC, Polymethylmethacrylate PMMA, Polyoxymethylene POM, and Polyethylene PE) were used as wall materials of the charging tube. To disperse and accelerate the particles, a gas flow rate of 3 m^3 h^{-1} was chosen. Further experimental setup of the charging tube involving a porous PE tube is used to facilitate air boundary-layer control (BLC) [40]. To prevent particle–wall interactions, different volume ratios (2.5% BLC I and 5% BLC II) of the total gas flow were radially inserted in the charging tube. An electrical field strength of 109 V/m was applied to the parallel-plate capacitor in the rectangular separation chamber

(46 mm × 52 mm × 400 mm). Binary protein-starch mixtures with protein contents of 15 wt. %, 30 wt. %, and 45 wt. % were used for the experiments. To determine the separation selectivity, the protein content on the anode and the cathode was measured by the absorption of protein at 280 nm on each electrode [36,39].

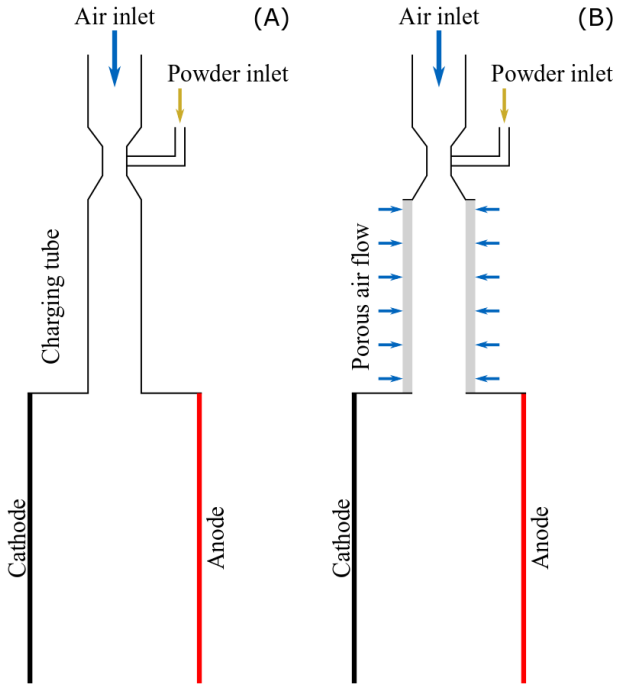

Figure 1. Scheme of the used dispersing, charging and separation setup with plain wall (**A**) and porous tube to adjust boundary-layer control (**B**). After the charging tube, particles are separated in a homogenous electrical field and particles are precipitated on the electrodes.

Triboelectric charging may occur when surfaces get into contact and are subsequently separated. Therefore, it is impossible to use uncharged particles to carry out experiments or to determine the charge of the particles before the experiments in a non-invasive manner. For the used powder containing starch and protein particles below 40 µm, the determination or even estimation of the charge of single particles is very challenging [41] and an interconnection of both experiments without altering the separation characteristics seems to be impossible. Thus, powder preparation and all experiments were carried out according to the same protocol to induce reproducible charge until the start of the experiment.

2.2.2. Particle Analysis

Particle size analysis for initial powders and the powder deposits on the electrodes were performed using the laser diffraction system (HELOS, Sympatec, Germany) with a measuring range of 0.25 µm to 87.5 µm and the wet dispersing unit QUIXEL. Ethanol was used as dispersion medium. The true density of each powder is evaluated using a gas pycnometer (Accupyc 1330, Micromeritics Instrument Corp., Norcross, GA, USA). Scanning electron microscopy (SEM) images of separated powders were recorded at an acceleration voltage of 5 kV (JSM-IT100, JEOL Ltd., Tokyo, Japan).

2.2.3. Particle Interaction Parameter

According to the particle size and flow conditions, the contact number of particles in a fluid can be estimated [42,43]. The encounter frequency γ of two particles with the diameters x_i and x_j in turbulent flow with the turbulence eddy dissipation rate ϵ and the viscosity of the fluid ν can be estimated according to Saffman and Turner [44], as follows:

$$\gamma = \frac{1.3}{8} \sqrt{\frac{\epsilon}{\nu}} (x_i + x_j)^3. \quad (1)$$

The contact of particles x in a binary powder mixture can occur between particles of different material and of different sizes. The turbulence eddy dissipation rate ϵ is taken from the results of the CFD study carried out in [36]. Furthermore, different powder mixtures vary in the protein to starch ratio and have a different number of particles for each species in the same size range. Thus, the encounter frequency must be scaled by the particle number in order to obtain a contact number depending on the particle size and the initial powder composition. The contact number Γ of each powder is calculated by the encounter frequency γ, scaled with the particle number of each size range c_i, c_j, and the mean interaction time Δt equivalent to the residence time of a particle in the charging tube [45]:

$$\Gamma = \frac{1.3}{8} \sqrt{\frac{\epsilon}{\nu}} \, \Delta t \, \sum_{i=1}^{n} \sum_{j=1}^{n} (x_i + x_j)^3 \, c_i \, c_j. \quad (2)$$

The particle number of each size range c_i, c_j is calculated using the measured particle size distribution and the true density of each powder. The size ranges i, j were taken from the used laser-diffraction system, whereby $n = 31$ classes are equally distributed on a logarithmic (base 10) scale.

Besides flow conditions, particle concentration, and particle size the charge of particles influences the contact number. Due to the charge, attractive and repulsive forces can result in segregation or agglomeration of particles, respectively, and therefore reduced contact numbers of particles. To understand the segregation or agglomeration of particles caused by triboelectric charging, several experimental and simulative studies were carried out [46–49]. However, in order to be able to apply the suggested models for calculating the contact number by electrostatic forces, the particle size-dependent charge distribution must be known, or the segregation or agglomeration within the charging section has to be determined. So far, the particle size-dependent charge distribution was not determined for such fine particles and seems to be challenging [41]. The determination of the segregation or agglomeration of particles within the charging tube for particles below 40 µm and flow velocity of $10\,\mathrm{m\,s^{-1}}$ is also challenging. In addition, agglomeration of particles due to electrostatic force is only investigated for very low gas velocities [47], and no agglomeration of particles was found in within same experimental conditions [50]. Therefore, electrostatic interaction is excluded for the estimation of contact number. Furthermore, a sensitivity analysis of the used equation to calculate the contact number is shown in Figure S1 (Supplementary Materials).

The calculation of the contact numbers of particles describes the initial and absolutely necessary step in triboelectric charging—the contact of two surfaces. However, triboelectric charging is a very complex phenomenon [5] and further factors like different materials, humidity, etc. play a decisive role. Since all experimental conditions are the same for each experiment, all random and unknown factors of triboelectric charging might be constant within this study. Hence, the contact numbers of particles are used to examine the influence of particle-particle-contacts and to cave out an influence parameter to engineer triboelectric charging.

2.2.4. Statistics

For all experiments the mean value was calculated from the results of three independent experiments ($n = 3$). The variance of the experiments are indicated by error bars. The error bars are calculated using Student's t-test at a significance level of $\alpha = 0.05$.

3. Results

3.1. Particle Size Distribution and SEM of Separated Powders

Figure 2 shows the particle size distribution of the raw materials, prepared powder mixtures (A), and separated powders on the cathode and anode (B). The protein powder has a monomodal particle

size distribution between 0.2 µm to 20 µm with a maximum value at 1 µm. The starch powder has a bimodal distribution with local maxima at 1 µm and 20 µm and a maximum particle size of 40 µm. Mixtures with initial protein contents of 15 wt. %, 30 wt. %, and 45 wt. % show similar particle size distributions with maximum values at 1 µm and 7 µm, because the particle size distributions of starch and protein overlap in almost the whole width. The particle size distribution could not be closed for all measured powders, because the used measuring range has enable both a detection of the largest and finest particles. Thus, particle sizes below 0.25 µm were neglected, since a dry dispersion of particles below 0.25 µm seems to be very unlikely. The particle size distributions of the separated powder show significantly different patterns on the cathode and the anode. On the anode, the particle size distributions show an approximately identical evolution for each initial protein content featuring almost the same peaks as starch, but with increased peak height. Therefore, the starch concentration on the anode is concluded to be high. In contrast, the particle size distributions of powders on the cathode bear a resemblance to the particle size distribution of the initial protein-starch mixture. Triboelectric separation leads to an increase in peak height at 1 µm and a flattening of the peak at larger particle sizes forming almost a monomodal distribution. Different initial protein contents lead to different peak heights at 1 µm; however, the shape of the particle size distributions above 4 µm is similar. The peak height is identical for the initial protein content of 30 wt. % and 45 wt. %, while both higher compared to 15 wt. %. Thus, separation efficiency depends on the initial protein content.

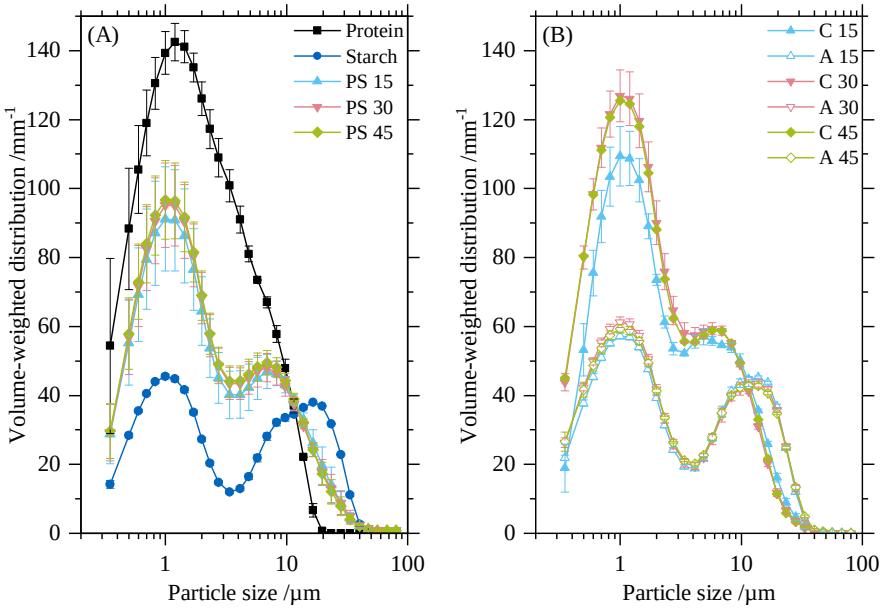

Figure 2. Particle size distributions of native powders, powder mixtures (**A**) and powders collected after separation (**B**) on cathode C (closed symbol) and anode A (open symbol). PVC was used as wall material in the charging tube. Despite varying protein content, initial powder mixtures have no different particle size distributions. On the cathode, an initially higher protein content results in finer powder. No such difference is visible on the anode.

Figure 3 shows SEM images of separated powders collected on the cathode (A) and anode (B) with an initial protein content of 30 wt. %. Small and rugged protein particles are clearly visible on the cathode. Protein particles tend to agglomerate among themselves forming larger structures. Only very few starch particles, identifiable by their round morphology and smooth surface, are detected on the cathode. On the contrary, starch particles of several sizes are found in very high incidence on the anode and very small protein particles are adsorbed on the surface of the starch particles. Thus, a complete separation of the powder mixture in starch and protein could not be achieved.

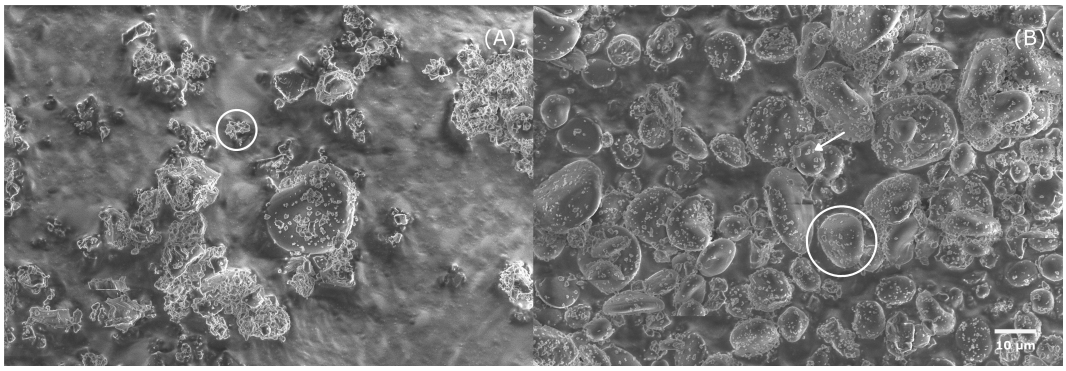

Figure 3. SEM images of separated powders on the cathode (**A**) and anode (**B**) with PVC as charging tube material. On the cathode, small and rugged protein particles (circle left) represent the main fraction. Smooth starch particles (circle right) predominate the population on the anode, while small protein particles adhere on the surface of large starch particles (arrow).

3.2. Influence on Separation Selectivity

Figure 4 shows the protein content indicating the separation selectivity on the cathode and anode after triboelectric separation. The protein content of the powder mixture was incrementally increased from 15 wt. % to 30 wt. % and 45 wt. %. Different wall materials were used to determine the combined influence of the particle-wall interaction and powder composition. For all employed wall materials, the increase in the initial protein content from 15 wt. % to 30 wt. % causes a significant increase in the protein content on the cathode, while the protein content on the anode remains unaffected. Such low protein contents on the anode indicate a very high starch content of up to 100 wt. %. Further increase in the initial protein content to 45 wt. % does not lead to an increase in the protein content on the cathode in combination with any of the tested contact materials. Thus, an increase in selectivity is observed only for PE and PVC. The tube materials POM and PMMA show no increase in selectivity above 30% protein content. In contrast, the protein content on the anode increases slightly when the initial protein content increases from 30 wt. % to 45 wt. % for all materials except PE. In summary, different wall materials have an impact on the selectivity at different initial protein contents; however, this impact cannot be explained on the basis of the empirical triboelectric series.

To test the influence of particle-wall interactions on triboelectric charging, wall contact was prevented by a boundary-layer control setup. A porous tube was applied with two different gas flow rates perpendicular to the particle stream [36]. The protein content on the cathode increases with the incremental increase in the initial protein content from 15 wt. % to 45 wt. %. The significant difference between 15 wt. % and 45 wt. % is in contrast to the plain wall setup. At the initial protein content of 15 wt. %, however, no significant differences between all BLC conditions are visible at the initial protein content of 15 wt. %. BLC I and BLC II show a small difference at 30 wt. %. At the highest initial protein content, no difference between BLC I, II and most of the plain wall setups was detected. On the anode, the protein content of BLC I and II increases as the initial protein content increases. Furthermore, only slight differences between the experimental setups were observed at 30 wt. %.

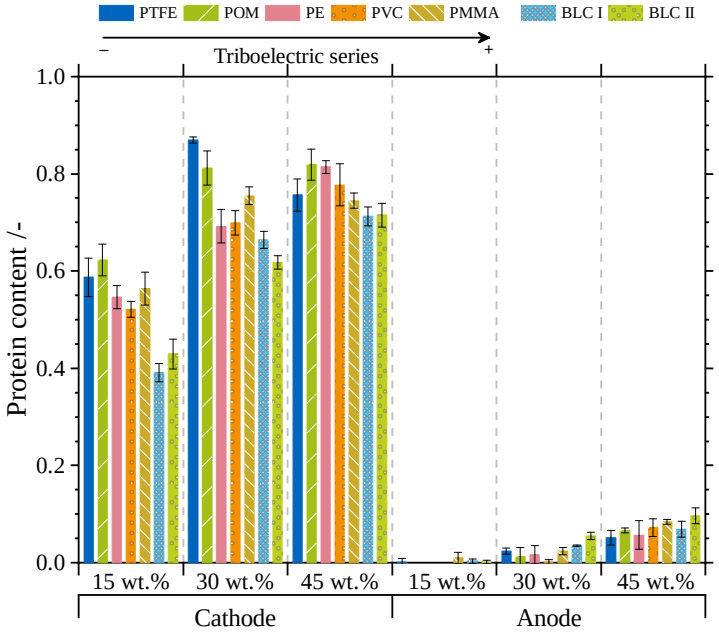

Figure 4. Protein content on the cathode and anode of powders with an initial protein content of 15 wt. %, 30 wt. % and 45 wt. %. Bars indicate different contact materials along with the triboelectric series and setup without wall interaction (BLC I & II). An increase in initial protein content leads to a significant increase in protein content on the cathode and anode. Different contact materials do not affect the protein content on each electrode. Results for 15 wt. % were taken from a previous study [36].

3.3. Particle Interaction

3.3.1. Contact Number Distribution Depending on Particle Size

Figure 5 shows the contact number distribution of protein (A) and starch (B) particles. The used values to calculate the contact numbers are summarised in Table 1. Protein particles show a high contact number for small particles. The contact number decreases as the particle size increases. The protein-protein contact number is always higher than the protein-starch contact number. An increase in protein content leads to an increase in the contact number for protein-protein and protein-starch. Starch particles show a high contact number for particles between 7 µm to 40 µm. The contact number between starch-protein increases by decreasing starch content in the initial powder mixture. These findings result from the increase in protein particle number because protein particles are a slightly finer than starch particles. The contact number between starch particles is almost the same for all investigated powder mixtures and always lower than the contact number between protein-starch. By comparing starch-starch and protein-protein contacts, the contact number of protein-protein interaction is always higher than that of starch-starch interaction. In summary, the variation in initial powder composition leads to different contact between the dispersed powders and thus might provide the first indication to the different separation selectivity (cf. Figure 4).

Table 1. Parameters used to calculate contact numbers of particles.

	Mean of Plain Wall	BLC I	BLC II
ϵ /m^2 s^{-3}	3.53×10^4	3.11×10^4	2.55×10^4
ν /m^2 s^{-1}		1.33×10^{-5}	
ρ_{Protein} /kg m^{-3}		1330	
ρ_{Starch} /kg m^{-3}		1520	

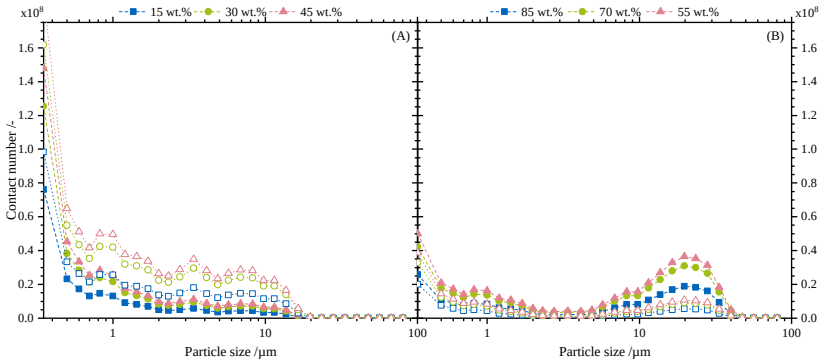

Figure 5. Contact number distribution of protein (**A**) and starch (**B**) particles. Closed symbols indicate the interaction with different materials, whereas open symbols show interaction with the same material. Protein shows a higher contact number for small particles. A higher initial protein content leads to higher contact numbers.

3.3.2. Separation Selectivity and Contact Numbers

A variation in the flow conditions leads to a change in the turbulence eddy dissipation rate, which plays a vital role in the contact number (Equation (1)). The experiments carried out with a plain wall, BLC I, and II have slightly different flow profiles. Thus, both a variation in the flow properties and that in the initial powder composition (cf. Figure 5) result in different contact numbers. As triboelectric or contact charging occurs, only a single contact suffices to attain a charged surface of a particle [29,37]. A collision of contrary charged particles of course results in charge annihilation. Based on this understanding, Figure 6 shows the protein content on the anode and cathode with respect to the contact number. The protein content on the cathode (closed symbols) shows a significant increase by increasing the contact number of particles. Lower contact numbers result in protein contents between 0.4 and 0.6, whereas higher contact numbers have protein contents of approximately 0.8. An increase in the protein content on the anode (open symbols) is also caused by an increase in the contact number. However, the increase in the protein content on the anode is considerably less compared to that on the cathode. For low contact numbers that have no protein can be detected on the anode, whereas for higher contact numbers, the maximum protein content reaches a value of 0.1. In summary, contact number affects the protein content on the anode and the cathode, while the protein content on the cathode is strongly affected and that on the anode is slightly affected.

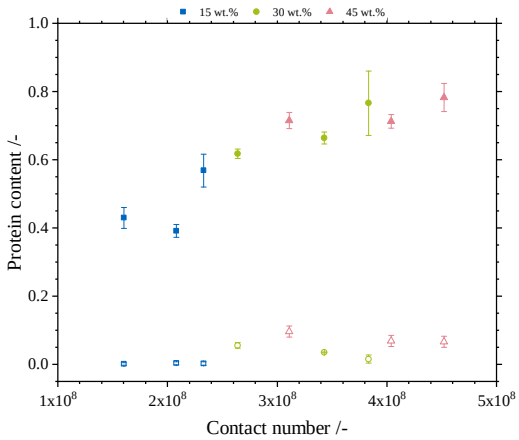

Figure 6. Protein content of separated powders on the cathode (closed symbols) and on the anode (open symbols). To improve clarity, the average protein content is plotted for all plain wall measurements. An increase in contact number results in a significant increase in protein content on the cathode. The protein content on the anode increases slightly with the increase in contact number.

4. Discussion

Triboelectric separation is a suitable technique used to separate powders containing different ratios of protein and starch [36,39,51–54]. The separation feature is not the particle size, as the particle size distributions of protein and starch overlap almost in the whole. Furthermore, there is no apparent dependency on the particle size during and after separation [50]. Powders containing different initial protein contents have similar particle size distributions before separation. After separation, the particle size distribution of the powders collected on the anode commonly shows the same evolution independent of the initial protein content. This underpins the independence of triboelectric separation from the particle size in a size range of 0.1 µm to 40 µm and puts the focus on the chemical composition [21] as well as further particle properties such as morphology and roughness as separation feature [25,27]. These results are in contrast with findings of the bipolar charging of single component powders claiming that small particles are always charged negatively [22,55–57].Furthermore, there are different charge distributions for positively and negatively charged particles [41]. The particle size distributions of powders collected on the cathode after separation feature higher peaks at 1 µm for initial protein contents of 30 wt. % and 45 wt. % compared to 15 wt. % (Figure 2). This increase can be associated with the increase in the protein content for higher initial protein concentrations. In contrast, the particle size distributions remain similar, implying an increase in the protein content on the anode with the stepwise increase in the initial protein content (Figure 4). However, comparing the particle size distribution of the pristine starch powder and the powder collected on the anode, a clear increase in the peak value of both peaks is visible, which might correspond to agglomerated particles on the electrodes, because no agglomeration was found for dispersed particles [50].

The separation selectivity shows a dependence on the initial protein content (Figure 4). For all plain wall setups and BLC setups, the protein content on the cathode increases with an increase in the initial protein content. Furthermore, all plain wall setups show no dependence on the triboelectric series of the wall materials. These findings correspond to the previous study [36]. As triboelectric charging can only occur if particles get into contact and are subsequently separated, the interactions of particles in the charging tube play a decisive role. Therefore, according to Saffman and Turner [44], an interaction parameter Γ of particles in a turbulent flow is calculated. In a binary powder mixture, a particle can collide with a particle of the same origin or with a particle of the other origin assuming that the particle-wall interaction plays a subordinated role. In addition to the origin of particles, the particle size affects the contact number of particles (Equation (2), Figure 5). Starch particles collide more frequently with protein particles, whereas protein particles collide more frequently among themselves. These findings indicate the influence of the pristine particle sizes as well as the initial protein content on triboelectric charging. Next to particle size and mixture composition, the flow properties in the charging tube also have an impact on the contact number. As Figure 6 shows, the contact number affects triboelectric separation properties which are in direct relation with triboelectric charging. The increase in the protein content on the cathode is accompanied by an almost linear increase along the particle-particle contact number. Since higher contact numbers of particles result in higher protein contents on the cathode, the protein content on the anode might decrease; however, on the anode the protein content is slightly increasing with increasing contact number. These findings might correlate with the increased interaction beneath protein particles (Figure 5). The increase of protein content on the anode due to higher contact numbers is huge compared with the increase of protein content on the anode. Therefore it is concluded, the increase in contact numbers of particles results in superior separation selectivity of fine organic powders. Thus, particle-particle interaction in the charging step of triboelectric separation is the decisive interaction parameter and can be used to enlarge or adjust triboelectric separation properties. Hence, the hypothesis that higher particle-particle contact numbers induced by a variation of the initial powder composition and turbulent flow profiles improves triboelectric separation selectivity is confirmed; however the calculation of the contact numbers of particles showed that powder composition mainly influence contact numbers and, thus, separation selectivity.

5. Conclusions

This study examines the influence of protein content in a binary powder mixture and flow properties on separation selectivity of triboelectric charging. The particle size distributions of initial and separated powder on the cathode showed an increase of fine particles with increasing initial protein content; however, the particle size distributions on the anode were unaffected by the initial protein content. These findings match with the separation selectivity. Thus, higher proportions of protein in the initial powder result in an increase of the protein content on both cathode and anode. Different wall materials along the empirical triboelectric series show no influence on the separation selectivity. A variation in the powder mixture and flow profile induce different contact numbers. An increase in the contact number results in an increase in the protein content. To put all in a nutshell, triboelectric charging and, thus, the separation selectivity of a binary powder mixture in turbulent flow can be influenced by the contact number of the particles. To adjust the contact number of particles, both particle size and turbulence eddy dissipation can be used. Thus, the contact number is a good parameter to improve triboelectric separation selectivity.

Supplementary Materials: The following are available online at http://www.mdpi.com/2227-9717/7/10/716/s1. Figure S1: Sensitivity analysis of Equation (2) to estimate the influence of turbulence eddy dissipation rate and protein content in the initial powder (from 0.99 to 0.01) on the contact number. Contact numbers and turbulent eddy dissipation rates used in this study are highlighted.

Author Contributions: J.L. did the conception and design of the study, the experimental work, and wrote the manuscript. P.F. participated to the writing and supervised the work.

Funding: This research received no external funding.

Acknowledgments: The authors would like to thank Stefan Schmideder for the fruitful discussion of contact number calculation and Heiko Briesen for the possibility to carry out this study.

Conflicts of Interest: The authors declare no conflict of interest.

Abbreviations

The following abbreviations are used in this manuscript:

BLC Bondary-layer control

References

1. Lacks, D.J.; Mohan Sankaran, R. Contact electrification of insulating materials. *J. Phys. D Appl. Phys.* **2011**, *44*, 453001.[CrossRef]
2. Matsusaka, S.; Masuda, H. Electrostatics of particles. *Adv. Powder Technol.* **2003**, *14*, 143–166.[CrossRef]
3. Matsusaka, S.; Maruyama, H.; Matsuyama, T.; Ghadiri, M. Triboelectric charging of powders: A review. *Chem. Eng. Sci.* **2010**, *65*, 5781–5807.[CrossRef]
4. Baytekin, H.T.; Patashinski, A.Z.; Branicki, M.; Baytekin, B.; Soh, S.; Grzybowski, B.A. The mosaic of surface charge in contact electrification. *Science* **2011**, *333*, 308–312.[CrossRef] [PubMed]
5. Lacks, D.J.; Shinbrot, T. Long-standing and unresolved issues in triboelectric charging. *Nat. Rev. Chem.* **2019**, *3*, 465–476.[CrossRef]
6. Grosshans, H.; Papalexandris, M.V. Large Eddy simulation of triboelectric charging in pneumatic powder transport. *Powder Technol.* **2016**, *301*, 1008–1015.[CrossRef]
7. Bunchatheeravate, P.; Curtis, J.; Fujii, Y.; Matsusaka, S. Prediction of particle charging in a dilute pneumatic conveying system. *AChE J.* **2013**, *59*, 2308–2316.[CrossRef]
8. Fotovat, F.; Bi, X.T.; Grace, J.R. Electrostatics in gas-solid fluidized beds: A review. *Chem. Eng. Sci.* **2017**, *173*, 303–334.[CrossRef]
9. Naik, S.; Mukherjee, R.; Chaudhuri, B. Triboelectrification: A review of experimental and mechanistic modeling approaches with a special focus on pharmaceutical powders. *Int. J. Pharm.* **2016**, *510*, 375–385.[CrossRef] [PubMed]

10. Mareev, E.A.; Dementyeva, S.O. The role of turbulence in thunderstorm, snowstorm, and dust storm electrification. *J. Geophys. Res. Atmos.* **2017**, *122*, 6976–6988.[CrossRef]
11. Forward, K.M.; Lacks, D.J.; Sankaran, R.M. Particle-size dependent bipolar charging of Martian regolith simulant. *Geophys. Res. Lett.* **2009**, *36*, 139.[CrossRef]
12. Lee, V.; Waitukaitis, S.R.; Miskin, M.Z.; Jaeger, H.M. Direct observation of particle interactions and clustering in charged granular streams. *Nat. Phys.* **2015**, *11*, 733–737.[CrossRef]
13. Dwari, R.K.; Mohanta, S.K.; Rout, B.; Soni, R.K.; Reddy, P.; Mishra, B.K. Studies on the effect of electrode plate position and feed temperature on the tribo-electrostatic separation of high ash Indian coking coal. *Adv. Powder Technol.* **2015**, *26*, 31–41.[CrossRef]
14. Mohanta, S.K.; Rout, B.; Dwari, R.K.; Reddy, P.; Mishra, B.K. Tribo-electrostatic separation of high ash coking coal washery rejects: Effect of moisture on separation efficiency. *Powder Technol.* **2016**, *294*, 292–300.[CrossRef]
15. Bouhamri, N.; Zelmat, M.E.; Tilmatine, A. Micronized plastic waste recycling using two-disc tribo-electrostatic separation process. *Adv. Powder Technol.* **2019**, *30*, 625–631.[CrossRef]
16. Messafeur, R.; Mahi, I.; Ouiddir, R.; Medles, K.; Dascalescu, L.; Tilmatine, A. Tribo-electrostatic separation of a quaternary granular mixture of plastics. *Part. Sci. Technol.* **2019**, *37*, 760–765.[CrossRef]
17. Xing, Q.; de Wit, M.; Kyriakopoulou, K.; Boom, R.M.; Schutyser, M.A. Protein enrichment of defatted soybean flour by fine milling and electrostatic separation. *Innov. Food Sci. Emerg. Technol.* **2018**, *50*, 42–49.[CrossRef]
18. Chen, Z.; Liu, F.; Wang, L.; Li, Y.; Wang, R.; Chen, Z. Tribocharging properties of wheat bran fragments in air–solid pipe flow. *Food Res. Int.* **2014**, *62*, 262–271.[CrossRef]
19. Albrecht, V.; Janke, A.; Drechsler, A.; Schubert, G.; Németh, E.; Simon, F. Visualization of Charge Domains on Polymer Surfaces. In *Characterization of Polymer Surfaces and Thin Films*; Progress in Colloid and Polymer Science; Grundke, K., Stamm, M., Adler, H.J., Eds.; Springer: Berlin/Heidelberg, Germany, 2006; Volume 132, pp. 48–53.
20. Harper, W.R. The Volta Effect as a Cause of Static Electrification. *Proc. R. Soc. A Math. Phys. Eng. Sci.* **1951**, *205*, 83–103.[CrossRef]
21. Kamiyama, M.; Maeda, M.; Okutani, H.; Koyama, K.; Matsuda, H.; Sano, Y. Effect of functional groups on the triboelectric charging property of polymer particles. *J. Appl. Polym. Sci.* **1994**, *51*, 1667–1671.[CrossRef]
22. Forward, K.M.; Lacks, D.J.; Sankaran, R.M. Triboelectric Charging of Granular Insulator Mixtures Due Solely to Particle—Particle Interactions. *Ind. Eng. Chem. Res.* **2009**, *48*, 2309–2314.[CrossRef]
23. Trigwell, S.; Grable, N.; Yurteri, C.U.; Sharma, R.; Mazumder, M.K. Effects of surface properties on the tribocharging characteristics of polymer powder as applied to industrial processes. *IEEE Trans. Ind. Appl.* **2003**, *39*, 79–86.[CrossRef]
24. Schönert, K.; Eichas, K.; Niermöller, F. Charge distribution and state of agglomeration after tribocharging fine particulate materials. *Powder Technol.* **1996**, *86*, 41–47.[CrossRef]
25. Atroune, S.; Tilmatine, A.; Alkama, R.; Samuila, A.; Dascalescu, L. Comparative Experimental Study of Triboelectric Charging of Two Size Classes of Granular Plastics. *Part. Sci. Technol.* **2015**, *33*, 652–658.[CrossRef]
26. Lacks, D.J.; Levandovsky, A. Effect of particle size distribution on the polarity of triboelectric charging in granular insulator systems. *J. Electrost.* **2007**, *65*, 107–112.[CrossRef]
27. Mukherjee, R.; Gupta, V.; Naik, S.; Sarkar, S.; Sharma, V.; Peri, P.; Chaudhuri, B. Effects of particle size on the triboelectrification phenomenon in pharmaceutical excipients: Experiments and multi-scale modeling. *Asian J. Pharm. Sci.* **2016**, *11*, 603–617.[CrossRef]
28. Sakaguchi, M.; Shimada, S.; Kashiwabara, H. Mechanoions produced by mechanical fracture of solid polymer. 6. A generation mechanism of triboelectricity due to the reaction of mechanoradicals with mechanoanions on the friction surface. *Macromolecules* **1990**, *23*, 5038–5040.[CrossRef]
29. Horn, R.G.; Smith, D.T.; Grabbe, A. Contact electrification induced by monolayer modification of a surface and relation to acid–base interactions. *Nature* **1993**, *366*, 442–443.[CrossRef]
30. Kolehmainen, J.; Sippola, P.; Raitanen, O.; Ozel, A.; Boyce, C.M.; Saarenrinne, P.; Sundaresan, S. Effect of humidity on triboelectric charging in a vertically vibrated granular bed: Experiments and modeling. *Chem. Eng. Sci.* **2017**, *173*, 363–373.[CrossRef]
31. Wistuba, H. The effect of an external electric field on the operation of an aluminium oxide–cast iron sliding contact joint. *Wear* **1997**, *208*, 113–117.[CrossRef]

32. Watanabe, H.; Ghadiri, M.; Matsuyama, T.; Maruyama, H.; Matsusaka, S.; Ghadiri, M.; Matsuyama, T.; Ding, Y.L.; Pitt, K.G.; Maruyama, H.; et al. Triboelectrification of pharmaceutical powders by particle impact. *Int. J. Pharm.* **2007**, *334*, 149–155.[CrossRef] [PubMed]
33. Ireland, P.M. Impact tribocharging of soft elastic spheres. *Powder Technol.* **2019**, *348*, 70–79.[CrossRef]
34. Ghori, M.U.; Supuk, E.; Conway, B.R. Tribo-electric charging and adhesion of cellulose ethers and their mixtures with flurbiprofen. *Eur. J. Pharm. Sci.* **2014**, *65*, 1–8.[CrossRef] [PubMed]
35. Murtomaa, M.; Laine, E. Electrostatic measurements on lactose–glucose mixtures. *J. Electrost.* **2000**, *48*, 155–162.[CrossRef]
36. Landauer, J.; Aigner, F.; Kuhn, M.; Foerst, P. Effect of particle-wall interaction on triboelectric separation of fine particles in a turbulent flow. *Adv. Powder Technol.* **2019**, *30*, 1099–1107.[CrossRef]
37. Horn, R.G.; Smith, D.T. Contact electrification and adhesion between dissimilar materials. *Science* **1992**, *256*, 362–364.[CrossRef] [PubMed]
38. Haeberle, J.; Schella, A.; Sperl, M.; Schröter, M.; Born, P. Double origin of stochastic granular tribocharging. *Soft Matter* **2018**, *14*, 4987–4995.[CrossRef] [PubMed]
39. Landauer, J.; Foerst, P. Triboelectric separation of a starch-protein mixture – Impact of electric field strength and flow rate. *Adv. Powder Technol.* **2018**, *29*, 117–123.[CrossRef]
40. Schlichting, H.; Gersten, K. *Boundary-Layer Theory*; Springer: Berlin/Heidelberg, Germay, 2017.[CrossRef]
41. Landauer, J.; Tauwald, S.M.; Foerst, P. A Simple\textmu-PTV Setup to Estimate Single-Particle Charge of Triboelectrically Charged Particles. *Front. Chem.* **2019**, *7*, 1.[CrossRef]
42. Meyer, C.J.; Deglon, D.A. Particle collision modeling—A review. *Miner. Eng.* **2011**, *24*, 719–730.[CrossRef]
43. Schmideder, S.; Kirse, C.; Hofinger, J.; Rollié, S.; Briesen, H. Modeling the Separation of Microorganisms in Bioprocesses by Flotation. *Processes* **2018**, *6*, 184.[CrossRef]
44. Saffman, P.G.; Turner, J.S. On the collision of drops in turbulent clouds. *J. Fluid Mech.* **1956**, *1*, 16.[CrossRef]
45. Smoluchowski, M. Versuch einer mathematischen Theorie der Koagulationskinetik kolloider Lösungen. *Z. Phys. Chem. (Leipzig)* **1917**, *92*, 129–168. [CrossRef]
46. Kolehmainen, J.; Ozel, A.; Boyce, C.M.; Sundaresan, S. Triboelectric charging of monodisperse particles in fluidized beds. *AIChE J.* **2017**, *63*, 1872–1891.[CrossRef]
47. Kolehmainen, J.; Ozel, A.; Gu, Y.; Shinbrot, T.; Sundaresan, S. Effects of Polarization on Particle-Laden Flows. *Phys. Rev. Lett.* **2018**, *121*, 124503.[CrossRef] [PubMed]
48. Schella, A.; Herminghaus, S.; Schröter, M. Influence of humidity on tribo-electric charging and segregation in shaken granular media. *Soft Matter* **2017**, *13*, 394–401.[CrossRef] [PubMed]
49. Schella, A.; Weis, S.; Schröter, M. Charging changes contact composition in binary sphere packings. *Phys. Rev. E* **2017**, *95*, 062903.[CrossRef] [PubMed]
50. Landauer, J.; Foerst, P. Influence of Particle Charge and Size Distribution on Triboelectric Separation—New Evidence Revealed by In Situ Particle Size Measurements. *Processes* **2019**, *7*, 381.[CrossRef]
51. Tabtabaei, S.; Jafari, M.; Rajabzadeh, A.R.; Legge, R.L. Solvent-free production of protein-enriched fractions from navy bean flour using a triboelectrification-based approach. *J. Food Eng.* **2016**, *174*, 21–28.[CrossRef]
52. Tabtabaei, S.; Jafari, M.; Rajabzadeh, A.R.; Legge, R.L. Development and optimization of a triboelectrification bioseparation process for dry fractionation of legume flours. *Sep. Purif. Technol.* **2016**, *163*, 48–58.[CrossRef]
53. Wang, J.; de Wit, M.; Boom, R.M.; Schutyser, M.A. Charging and separation behavior of gluten–starch mixtures assessed with a custom-built electrostatic separator. *Sep. Purif. Technol.* **2015**, *152*, 164–171.[CrossRef]
54. Wang, J.; de Wit, M.; Schutyser, M.A.; Boom, R.M. Analysis of electrostatic powder charging for fractionation of foods. *Innov. Food Sci. Emerg. Technol.* **2014**, *26*, 360–365.[CrossRef]
55. Inculet, I.I.; Peter Castle, G.S.; Aartsen, G. Generation of bipolar electric fields during industrial handling of powders. *Chem. Eng. Sci.* **2006**, *61*, 2249–2253.[CrossRef]

56. Zhao, H.; Castle, G.; Inculet, I.I.; Bailey, A.G. Bipolar charging of poly-disperse polymer powders in fluidized beds. *IEEE Trans. Ind. Appl.* **2003**, *39*, 612–618.[CrossRef]
57. Sowinski, A.; Miller, L.; Mehrani, P. Investigation of electrostatic charge distribution in gas–solid fluidized beds. *Chem. Eng. Sci.* **2010**, *65*, 2771–2781.[CrossRef]